



# Divergent Patterns of TDP-43 and Tau Pathologies in Primary Progressive Aphasia

Lucia A. A. Giannini, BS, BA <sup>1,2,3</sup> Sharon X. Xie, PhD,<sup>4</sup> Corey T. McMillan, PhD,<sup>1</sup> Mendy Liang, BS,<sup>1,2</sup> Andrew Williams, BS,<sup>1,2</sup> Charles Jester, BS,<sup>1</sup> Katya Rascovsky, PhD,<sup>1</sup> David A. Wolk, MD,<sup>5</sup> Sharon Ash, PhD,<sup>1</sup> Edward B. Lee, MD, PhD,<sup>6,7</sup> John Q. Trojanowski, MD, PhD,<sup>6</sup> Murray Grossman, MD,<sup>1</sup> and David J. Irwin, MD <sup>1,2</sup>

**Objective:** To measure postmortem burden of frontotemporal lobar degeneration (FTLD) with TDP-43 (FTLD-TDP) or tau (FTLD-Tau) proteinopathy across hemispheres in primary progressive aphasia (PPA) using digital histopathology and to identify clinicopathological correlates of these distinct proteinopathies.

**Methods:** In an autopsy cohort of PPA (FTLD-TDP = 13, FTLD-Tau = 14), we analyzed laterality and regional distribution of postmortem pathology, quantified using a validated digital histopathological approach, in available brain tissue from up to 8 cortical regions bilaterally. We related digital pathology to antemortem structural neuroimaging and specific clinical language features.

**Results:** Postmortem cortical pathology was left-lateralized in both FTLD-TDP (beta = -0.15, standard error [SE] = 0.05,  $p = 0.007$ ) and FTLD-Tau (beta = -0.09, SE = 0.04,  $p = 0.015$ ), but the degree of lateralization decreased with greater overall dementia severity before death (beta = -8.18, SE = 3.22,  $p = 0.015$ ). Among 5 core pathology regions sampled, we found greatest pathology in left orbitofrontal cortex (OFC) in FTLD-TDP, which was greater than in FTLD-Tau ( $F = 47.07$ ,  $df = 1,17$ ,  $p < 0.001$ ), and in left midfrontal cortex (MFC) in FTLD-Tau, which was greater than in FTLD-TDP ( $F = 19.34$ ,  $df = 1,16$ ,  $p < 0.001$ ). Postmortem pathology was inversely associated with antemortem magnetic resonance imaging cortical thickness (beta = -0.04, SE = 0.01,  $p = 0.007$ ) in regions matching autopsy sampling. Irrespective of PPA syndromic variant, single-word comprehension impairment was associated with greater left OFC pathology ( $t = -3.72$ ,  $df = 10.72$ ,  $p = 0.004$ ) and nonfluent speech with greater left MFC pathology ( $t = -3.62$ ,  $df = 12.00$ ,  $p = 0.004$ ) among the 5 core pathology regions.

**Interpretation:** In PPA, FTLD-TDP and FTLD-Tau have divergent anatomic distributions of left-lateralized postmortem pathology that relate to antemortem structural imaging and distinct language deficits. Although other brain regions may be implicated in neural networks supporting these complex language measures, our observations may eventually help to improve antemortem diagnosis of neuropathology in PPA.

ANN NEUROL 2019;00:1–14

In primary progressive aphasia (PPA), neurodegeneration of the perisylvian language network is most often caused by frontotemporal lobar degeneration (FTLD) pathologies.<sup>1,2</sup> Clinical syndromic variants of PPA have been associated

statistically with specific neuropathological substrates: the nonfluent/agrammatic variant (naPPA) with tauopathies (FTLD-Tau), the logopenic variant with Alzheimer disease (AD) pathology, and the semantic variant (svPPA) with

View this article online at [wileyonlinelibrary.com](http://wileyonlinelibrary.com). DOI: 10.1002/ana.25465

Received Dec 7, 2018, and in revised form Mar 6, 2019. Accepted for publication Mar 7, 2019.

Address correspondence to Dr Irwin, Frontotemporal Degeneration Center (FTDC), University of Pennsylvania Perelman School of Medicine, Hospital of the University of Pennsylvania, 3600 Spruce Street, Philadelphia, PA 19104. E-mail: [dirwin@penmedicine.upenn.edu](mailto:dirwin@penmedicine.upenn.edu)

From the <sup>1</sup>Penn Frontotemporal Degeneration Center, Department of Neurology, Perelman School of Medicine, University of Pennsylvania, Philadelphia, PA; <sup>2</sup>Digital Neuropathology Laboratory, Department of Neurology, Perelman School of Medicine, University of Pennsylvania, Philadelphia, PA;

<sup>3</sup>Department of Neurology, University Medical Center Groningen, University of Groningen, Groningen, the Netherlands; <sup>4</sup>Department of Biostatistics, Epidemiology, and Informatics, Perelman School of Medicine, University of Pennsylvania, Philadelphia, PA; <sup>5</sup>Alzheimer's Disease Center, Department of Neurology, Perelman School of Medicine, University of Pennsylvania, Philadelphia, PA; <sup>6</sup>Center for Neurodegenerative Disease Research, Department of Pathology and Laboratory Medicine, Perelman School of Medicine, University of Pennsylvania, Philadelphia, PA; and <sup>7</sup>Translational Neuropathology Research Laboratory, Department of Pathology and Laboratory Medicine, Perelman School of Medicine, University of Pennsylvania, Philadelphia, PA

FTLD with transactive response DNA binding protein of ~43 kDa (TDP-43) inclusions (FTLD-TDP).<sup>2,3</sup> However, these syndromic variants do not predict pathology with sufficient reliability for clinical trials, as FTLD-Tau with clinical svPPA or FTLD-TDP with clinical naPPA are not uncommon.<sup>3–5</sup> Moreover, many patients have features that overlap with different PPA variants,<sup>3,4</sup> making implementation of clinical criteria challenging even at specialized centers. Finally, AD pathology may mimic any of the PPA syndromes.<sup>3,4,6</sup> These factors limit the utility of current clinical variant criteria<sup>7</sup> for predicting underlying neuropathology.

The anatomic distribution of disease is highly influential for the clinical manifestations of PPA. Recent work has studied hemispheric and regional brain involvement in PPA variants using in vivo techniques of neuroimaging,<sup>8,9</sup> but postmortem studies characterizing regional pathology are very rare, and antemortem imaging is seldom cross-validated with postmortem pathologic burden. Left-hemisphere lateralization of cortical disease has been demonstrated in vivo<sup>10,11</sup> and confirmed qualitatively postmortem,<sup>3</sup> yet right-hemisphere disease appears to contribute to language deficits in antemortem imaging of autopsy-confirmed PPA.<sup>12</sup> Postmortem lateralization of pathology has been measured in limited PPA cases with FTLD-TDP,<sup>13–16</sup> whereas distribution of pathology in PPA with FTLD-Tau is understudied. Furthermore, despite the limited reliability of clinicopathological correlations using PPA syndromic variants, individual clinical features of PPA have only rarely been related to specific anatomic distributions of disease in patients with presumed proteinopathies during life,<sup>17,18</sup> or with a categorical neuropathological diagnosis.<sup>4,19</sup> Here we use a digital approach to perform a fine-grained comparative study of postmortem FTLD-TDP and FTLD-Tau proteinopathies in PPA, and integrate antemortem clinical features and structural magnetic resonance imaging (MRI) with digital pathology. We test the hypotheses that (1) postmortem pathology in PPA is lateralized to the left hemisphere regardless of molecular pathology; (2) FTLD-TDP and FTLD-Tau have divergent, pathology-specific patterns of disease; and (3) the anatomic distribution of pathology is related to distinct antemortem linguistic and imaging features in PPA.

## Materials and Methods

### Patients

Experienced cognitive neurologists (M.G., D.A.W., D.J.I.) evaluated patients at the Penn Frontotemporal Degeneration Center or Alzheimer's Disease Center, and selected cases meeting criteria from the Penn Integrated Neurodegenerative Disease Database.<sup>20</sup> We identified patients with FTLD pathologies that meet modern clinical PPA criteria<sup>1</sup> based on systematic chart review and extraction of clinical features by a consensus panel of experienced

investigators (C.T.M., D.A.W., D.J.I., K.R., L.A.A.G., M.G., S.A.) established prospectively and prior to neuropathological diagnosis. Details on patient inclusion/exclusion are described in Figure 1. Patients with primary AD pathology or medium/high-level secondary AD copathology were excluded. Our final cohort consisted of 27 PPA patients with autopsy-confirmed FTLD-TDP (n = 13) or FTLD-Tau (n = 14). We previously reported clinical and qualitative pathology data for 12 of these patients as a reference group for a study of PPA with AD pathology.<sup>4</sup> All procedures were performed with informed consent in accordance with the regulations of the Penn Institutional Review Board.

### Neuropathological Examination

Fresh tissue was sampled at autopsy in standardized regions for diagnosis and fixed overnight in 10% neutral buffered formalin.<sup>21</sup> Tissue was processed as described,<sup>22</sup> embedded in paraffin blocks and cut into 6  $\mu$ m sections for immunohistochemical staining for tau, A $\beta$ , TDP-43, and alpha-synuclein with well-characterized antibodies.<sup>21</sup> Neuropathological diagnosis was performed by expert neuropathologists (E.B.L., J.Q.T.) using established criteria.<sup>23,24</sup> Patients were classified based on primary neuropathological diagnosis as FTLD-TDP (ie, subtypes A, B, or C) or FTLD-Tau (ie, Pick disease [PiD], progressive supranuclear palsy [PSP], or corticobasal degeneration [CBD]).

### Genetic Analysis

Patients were genotyped for pathogenic mutations in *GRN*, *C9orf72*, and *MAPT* as described<sup>25</sup> based on family history risk from structured pedigree analysis.<sup>26</sup>

### Digital Image Analysis

For this study, we used tissue fixed in formalin in an identical manner as outlined above,<sup>21</sup> except for a minority of slides (n = 10) fixed in 70% ethanol with 150 mmol NaCl to supplement regions missing formalin-fixed tissue as previously validated.<sup>22</sup> Tissue was immunostained for phosphorylated TDP-43 (rat monoclonal TAR5P-1D3, p409/410; Ascension, Munich, Germany)<sup>27</sup> or tau (AT8; Millipore, Billerica, MA)<sup>28</sup> as described.<sup>22</sup> Digital image analysis was performed with Halo software v1.90 (Indica Labs, Albuquerque, NM) with validated sampling and thresholding algorithms for FTLD-TDP and FTLD-Tau.<sup>22</sup> We measured percentage of area occupied (%AO) by TDP-43 or tau inclusions in gray matter regions of interest (ROIs) as described.<sup>22,25</sup> To reduce batch effects of immunohistochemical staining, all slides were stained in the same batch or %AO measurements were transformed using linear regression derived from a subset of slides run in duplicate. We validated %AO scores by comparison to traditional ordinal scores (ie, 0–3), obtained blinded to quantitative pathology measurements, as previously done.<sup>22</sup>

Pathology data (see Fig 1) included 5 standard “core” regions, which were sampled from a random hemisphere at autopsy according to standardized National Institute on Aging/Alzheimer's Association diagnostic guidelines<sup>24</sup> in the total cohort. These core regions include anterior cingulate gyrus (ACG; Brodmann area [BA] 24), angular gyrus (ANG; BA 39), midfrontal cortex (MFC; BA 46), orbitofrontal cortex (OFC; BA

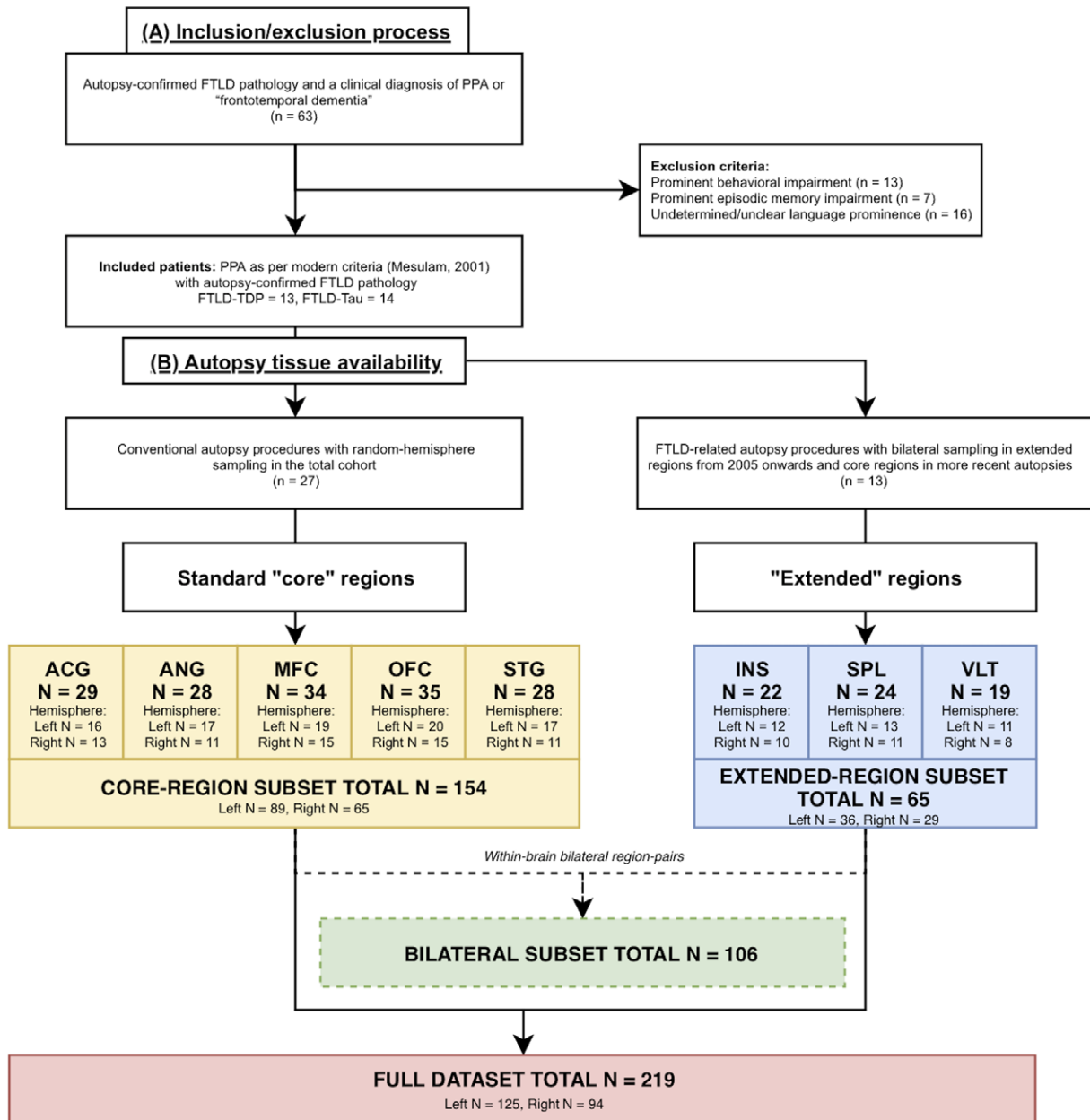


**FIGURE 1:** Flow-chart depicting patient inclusion/exclusion and pathology data availability. Flow-chart shows (A) our inclusion/exclusion process and (B) the final availability of autopsy tissue. (A) Of all patients with autopsy-confirmed frontotemporal lobar degeneration (FTLD) pathology and a clinical diagnosis of primary progressive aphasia (PPA) or "frontotemporal dementia" (n = 63) for those evaluated prior to modern criteria, we excluded those who did not qualify as PPA<sup>1</sup> because of prominent behavioral (n = 13) or episodic memory (n = 7) impairments, or insufficient evidence to verify prominence of language impairment at onset (n = 16). Our final cohort consisted of 27 patients, of whom 13 patients had FTLD with inclusions of the transactive response DNA-binding protein 43 (FTLD-TDP) and 14 patients had FTLD with inclusions of the tau protein (FTLD-Tau). (B) Available autopsy tissue included 5 standard "core" regions (ie, anterior cingulate gyrus [ACG], angular gyrus [ANG], midfrontal cortex [MFC], orbitofrontal cortex [OFC], superior-temporal gyrus [STG]), that is, regions that were sampled at autopsy in the total cohort following conventional autopsy procedures with random hemisphere sampling<sup>24</sup> (ie, core-region subset). Additionally, our laboratory recently expanded pathology protocols to improve the neuropathological characterization of patients with FTLD<sup>25</sup> by collecting tissue from both hemispheres in 3 "extended" regions (ie, insular cortex [INS], superior parietal lobule [SPL], ventrolateral temporal cortex [VLT]) in 13 recent PPA brains (ie, extended-region subset), and more recently implemented bilateral sampling in core regions as well. In total, we collected 219 tissue samples (ie, full dataset), comprising tissue from core (n = 154) and extended regions (n = 65), and including the subset of bilateral data with 106 matched left-right tissue samples (ie, bilateral subset). n = number of patients; N = number of slides.

11), and superior-temporal gyrus (STG; BA 22). Additional data were available from "extended" regions sampled from both hemispheres in autopsies since 2005 (FTLD-TDP = 5, FTLD-Tau =

8) to capture anatomic substrates associated with language and behavior in FTLD as described,<sup>25</sup> that is, anterior insular cortex (INS; BA 13), ventrolateral temporal cortex (VLT; BA 20), and

a control region less involved in FTLT, that is, superior parietal lobule (SPL; BA 5). We have 29 within-brain bilateral region-pairs from extended regions, and more recently we collected bilateral sampling in standard core regions as well, obtaining an additional set of 24 within-brain bilateral region-pairs. To analyze pathology burden between hemispheres across brain regions, we used all available bilateral data uniquely collected at our center (ie, bilateral subset), comprising 53 bilateral region-pairs for a total of 106 individual tissue samples. To analyze pathology burden between brain regions within each hemisphere, we used data from core regions sampled in all autopsies (ie, core-region subset), including 89 left-hemisphere and 65 right-hemisphere samples. Our total dataset including tissue from both standard core ( $n = 154$ ) and extended regions ( $n = 65$ ) amounted to 219 samples (ie, full dataset). Please see Figure 1 for an overview of available sampled tissue. Missing data and damaged tissues were excluded from analyses.

### Clinical Data

Available clinical records were reviewed blinded to neuropathological diagnosis. All patients had >1 visit with a comprehensive, formal language evaluation performed by an experienced cognitive neurologist at our outpatient cognitive neurology clinic using a validated protocol,<sup>29,30</sup> or similar bedside assessment in patients evaluated prior to modern PPA criteria. We abstracted the presence of clinical features systematically tested and reported in the record by the clinician as binary variables (ie, presence/absence of specific features) using a standardized chart review and discussed in a weekly consensus panel as described.<sup>4,25,31</sup> Nonfluent speech was defined as the presence of slowed and/or effortful speech with reduced word output as described.<sup>4,31</sup> Clinical data were categorized into early disease (0–3 years after onset) and late disease (>3 years after onset). Patients with missing data in early ( $n = 6$ ) or late ( $n = 7$ ) disease periods were excluded from these analyses. Patients were classified into clinical PPA variants when consistent with current criteria,<sup>7</sup> or defined as unclassifiable due to concurrent semantic and non-fluent/agrammatic features. Classification details for individual patients are specified in Table 1. Additionally, we retrospectively scored the sum of boxes of the extended Clinical Dementia Rating (CDR) scale including frontotemporal dementia (FTD)-related behavior and language subfields,<sup>32</sup> at first and last available visits.

### Neuroimaging

A subset of patients ( $n = 11$ ) had research-quality T1 structural MRI data. Quantitative MRI data were processed using ANTS.<sup>33,34</sup> We measured cortical thickness in each hemisphere using multiatlas segmentation with joint label fusion<sup>35</sup> in ROIs approximating regions sampled at autopsy, as described.<sup>22,25</sup> To determine cortical thinning in each ROI, we derived  $z$  scores based on a demographically comparable healthy control cohort without psychiatric or neurological history (male = 47, female = 66, average education = 16.0 years, average age = 65.2 years).

### Statistical Analysis

Categorical clinical features were compared between groups using Fisher exact test, whereas non-normally distributed demographic variables were compared using Mann–Whitney  $U$  test.

Neuropathology and neuroimaging data were tested using parametric statistics as described below. We used linear mixed effects (LME) modeling with random intercepts for individual patients to account for interdependency of multiple measurements from the same patient and for missing data.<sup>36</sup> To assess the effect of a multilevel categorical variable on the model, type III analysis of variance with Satterthwaite approximation was employed. Planned post hoc comparisons for LME outcomes were performed on LME-derived least-square means with Tukey correction for multiple comparisons. All analyses were 2-sided, with significance level set at 0.05, and were performed using R Statistical Software 3.4.1.

Because the absolute %AO varied due to differences in morphological inclusions,<sup>25</sup> %AO scores were scaled to a comparable range [0;1] (ie, normalized %AO) using min–max normalization:  $x' = (x - \min) / (\max - \min)$ . To maximize biological accuracy, this normalization step was performed within pathology subtypes (FTLD-TDP: type A/B, type C; FTLT-Tau: CBD, PiD, PSP).

Lateralization of pathology was tested using an LME analysis of normalized %AO across all available bilaterally sampled region-pairs (ie, bilateral subset) in FTLT-TDP and FTLT-Tau, covarying for disease duration at autopsy and mutation status in FTLT-TDP. For a direct measure of laterality, an asymmetry index (AI) was calculated in bilateral region-pairs using raw %AO scores<sup>25</sup>:  $AI = (\text{left \%AO} - \text{right \%AO}) / (\text{average left \%AO} \& \text{right \%AO}) \times 100$ . We tested regional AI with a 1-sample  $t$  test against the null-hypothesis that mean AI = 0 (ie, no lateralization), and we assessed the relationship between CDR score at last visit and AI using an LME model across all regions.

Within-group analysis of regional pathology was performed using an LME model testing the effect of region on normalized %AO in left- and right-hemisphere standard core regions (ie, core-region subset), covarying for disease duration at autopsy, and mutation status in FTLT-TDP. We defined greatest core-region pathology as the region with the highest least-square mean derived from LME modeling in each hemisphere in FTLT-TDP and FTLT-Tau. Between-group comparisons of pathology burden were performed using analysis of covariance with normalized %AO as outcome variable, covarying for disease duration at autopsy.

We tested the relationship between normalized %AO and MRI cortical thickness in the full dataset with an LME model comprising ROIs matching available regional pathology data, covarying for time from scan to autopsy. We used independent samples  $t$  tests to compare normalized %AO measurements in greatest core-pathology regions between patients with and without clinical language features characteristic of naPPA and svPPA.

## Results

### Clinical Characterization

The cohort comprised 13 patients with FTLT-TDP and 14 with FTLT-Tau (see Table 1), who did not differ in demographic characteristics. All but 2 patients were right-handed. FTLT-TDP and FTLT-Tau differed in the frequencies of clinical variants ( $p = 0.007$ , Fisher exact test). FTLT-TDP was associated with svPPA in 8 of 13 patients (61.5%), whereas 3 of 13 (23.1%) patients had naPPA

TABLE 1. Cohort Characteristics and Demographics

	ID	Sex	Education, yr	Handedness	PPA Variant	Path Subtype	Gene Mutation	Brain wt, g	PMI, h	Braak	CERAD	Age at Onset, yr	Disease Duration, yr	CDR First Visit <sup>a</sup>	CDR Last Visit <sup>a</sup>
FTLD-TDP	1	M	12	R	svPPA <sup>b</sup>	C		1,053	4	0	B	62	18.8	1.5	19
	2	F	12	R	svPPA	C		1,003	20	0	0	62	6.7	2.5	na
	3	M	20	L	svPPA	C		1,359	6	1	0	55	8.0	6.5	20
	4 <sup>c,d</sup>	F	18	R	svPPA <sup>c</sup>	A	<i>GRN</i>	790	8	0	0	56	5.7	14	23
	5 <sup>d</sup>	F	18	R	Unclas	A	<i>GRN</i>	742	4.5	1	0	52	10.5	10.5	17.5
	6 <sup>c,d</sup>	F	12	R	Unclas	A	<i>GRN</i>	1,055	8.5	1	0	65	3.5	4.5	23
	7	M	16	R	svPPA	C		1,390	16.5	1	A	62	10.3	4.5	9.5
	8	M	16	R	svPPA	C		1,060	20	0	0	65	11.4	3	21
	9 <sup>c</sup>	M	18	R	naPPA	A	<i>GRN</i>	866	18	1	0	56	10.3	4	22
	10 <sup>c</sup>	M	22	R	svPPA	A		1,090	16	1	0	59	11.6	3	13.5
	11	M	16	R	naPPA	A		1,160	6.5	0	0	52	3.4	3.5	21
	12	M	na	R	svPPA	C		1,157	12.5	0	0	50	13.5	1	11.5
	13 <sup>c</sup>	F	18	L	naPPA <sup>f</sup>	B		1,069	17	1	A	69	1.4	9	17.5
FTLD-Tau	14 <sup>c</sup>	F	12	R	naPPA	CBD		902	14	0	A	66	11.1	2	19
	15	F	16	R	naPPA	CBD		1,149	19.5	0	0	52	4.8	4.5	16
	16 <sup>d</sup>	F	12	R	naPPA	PSP		1,035	17	2	A	63	7.7	11.5	na
	17	M	20	R	Unclas	CBD		1,085	17	1	A	63	5.6	4	20
	18	M	12	R	naPPA	PSP		1,100	13	0	0	71	10.0	3.5	20
	19 <sup>c</sup>	F	16	R	naPPA	CBD		906	4	1	0	58	8.3	2	22
	20 <sup>c</sup>	M	20	R	svPPA	PiD		1,049	4	0	0	54	17.2	6	24
	21	F	12	R	naPPA	CBD		1,340	19	0	0	74	5.9	2	14
	22 <sup>c</sup>	F	16	R	Unclas	PiD		1,053	14	0	0	57	9.1	3.5	21
	23 <sup>c</sup>	M	na	R	naPPA	PSP		1,310	4	2	0	76	7.9	4.5	20.5
	24	F	na	R	Unclas	CBD		1,080	15	0	0	65	5.7	2	20
	25	M	16	R	naPPA	PSP		1,014	15.5	1	A	67	5.7	4.5	na
	26 <sup>d</sup>	M	16	R	naPPA	PSP		1,297	5	1	0	70	9.6	5	15.5
	27 <sup>c</sup>	F	16	R	naPPA	CBD		1,162	10	1	A	58	9.5	2.5	8

<sup>a</sup>The CDR scale was scored at first available visit for all patients, and at last visit for patients with >1 available visits.

<sup>b</sup>Patient 1 had a logopenic presentation in early disease (lvPPA–, ie, meeting ancillary clinical features of lvPPA but not core features due to preserved repetition<sup>4</sup>), and progressed to an svPPA phenotype as per clinical criteria.

<sup>c</sup>These patients (n = 11) had available antemortem magnetic resonance imaging data.

<sup>d</sup>Low levels of secondary copathologies were present in a minority of patients with no or rare cortical involvement. Patients 4 and 5 had hippocampal sclerosis. Patient 6 had secondary argyrophilic grain disease with rare cortical pathology. Patients 16 and 26 had secondary Lewy body disease (limbic stage).

<sup>e</sup>Patient 4 met core criteria for svPPA, but there was insufficient data to determine whether this patient fulfilled ancillary svPPA criteria.

<sup>f</sup>Patient 13 had naPPA at onset and thereafter developed motor neuron disease features leading to a diagnosis of amyotrophic lateral sclerosis.

A–C = FTLD-TDP subtypes according to current neuropathological criteria<sup>23</sup>; CBD = corticobasal degeneration; CDR = Clinical Dementia Rating including frontotemporal dementia (FTD) subfields<sup>32</sup>; CERAD = Consortium to Establish a Registry for Alzheimer's Disease; F = female; FTLD-Tau = frontotemporal lobar degeneration with inclusions of the tau protein; FTLD-TDP = frontotemporal lobar degeneration with inclusions of the transactive response DNA-binding protein 43; *GRN* = progranulin gene; L = left-handed; lvPPA = logopenic PPA; M = male; na = not available; naPPA = nonfluent/agrammatic variant of PPA; PiD = Pick disease; PMI = postmortem interval; PPA = primary progressive aphasia; PSP = progressive supranuclear palsy; R = right-handed; svPPA = semantic variant of PPA; Unclas = unclassifiable primary progressive aphasia with concurrent nonfluent/agrammatic and semantic features; wt = weight.

and 2 of 13 (15.4%) had an unclassifiable phenotype with mixed semantic and nonfluent/agrammatic features. FTLD-Tau was associated with naPPA in 10 of 14 patients (71.4%), whereas 1 of 14 (7.1%) had svPPA, and 3 of 14 (21.4%) were unclassifiable. Four FTLD-TDP patients carried a *GRN* mutation. Likewise, 8 of 9 (88.9%) svPPA patients had FTLD-TDP pathology, whereas 10 of 13 (76.9%) naPPA patients had FTLD-Tau pathology. Thus, clinical syndromes did not consistently predict expected pathology, and 5 of 27 (18.5%) patients could not be classified due to mixed features.

We compared clinical language features between FTLD-TDP and FTLD-Tau independently of clinical syndrome (Table 2; statistics: Fisher exact test). In early disease (0–3 years after onset), 9 of 10 (90.0%) FTLD-Tau patients had nonfluent speech, which was more frequent than 4 of 11 (36.4%) patients with FTLD-TDP ( $p = 0.024$ ), and impairment of single-word comprehension in 7 of 10 (70.0%) patients with FTLD-TDP approached significance when compared to 2 of 9 (22.2%) patients with FTLD-Tau ( $p = 0.070$ ). In late disease (>3 years after onset), 11 of 12 (91.7%) of FTLD-Tau patients had nonfluent speech compared to 2 of 8 (25.0%) with FTLD-TDP ( $p = 0.004$ ). Additionally, FTLD-Tau patients had higher frequency of agrammatism ( $p = 0.005$ ), dysarthria ( $p = 0.028$ ), phonemic paraphasias ( $p = 0.019$ ), and impaired sentence repetition ( $p = 0.018$ ) than FTLD-TDP patients. Conversely, 7 of 7 (100.0%) patients with FTLD-TDP in late disease had single-word comprehension difficulties, greater than 5 of 12 (41.7%) in FTLD-Tau patients ( $p = 0.017$ ), and were more often impaired in object knowledge ( $p = 0.009$ ) and meaningful content of speech ( $p = 0.019$ ) than FTLD-Tau patients. Thus, distinctive language features, that is, nonfluent speech in FTLD-Tau and impaired single-word comprehension in FTLD-TDP, were relatively more reliable than syndromic variants.

### Neuropathological Analysis: Lateralization

We studied the interhemispheric distribution of TDP-43 and tau across all bilaterally sampled region-pairs. Cortical pathology was lateralized to the left hemisphere in both FTLD-TDP (beta =  $-0.15$ , standard error [SE] =  $0.05$ ,  $p = 0.007$ ) and FTLD-Tau (beta =  $-0.09$ , SE =  $0.04$ ,  $p = 0.015$ ). The 2 left-handed patients of our cohort did not have bilateral sampling and were not included in this analysis.

We used the AI as a direct measure of laterality in each region (Fig 2A). FTLD-TDP showed region-specific left lateralization of OFC (mean AI =  $60.9 \pm 41.0$ ,  $t = 3.32$ ,  $df = 4$ ,  $p = 0.029$ ) and SPL (mean AI =  $150.9 \pm 55.6$ ,  $t = 4.70$ ,  $df = 2$ ,  $p = 0.042$ ), whereas FTLD-Tau had region-specific left lateralization of MFC (mean AI =  $79.0 \pm 46.8$ ,  $t = 3.37$ ,  $df = 3$ ,  $p = 0.043$ ). Furthermore, AI was negatively associated with full CDR at last visit

(beta =  $-8.18$ , SE =  $3.22$ ,  $p = 0.015$ ) across all regions and irrespective of pathology group (see Fig 2B), suggesting that increased overall clinical dementia severity before death was associated with reduced left lateralization of pathology.

### Neuropathological Analysis: Within-Group Regional Burden

We analyzed within-group regional burden of pathology in the 5 standard core regions. In left-hemisphere FTLD-TDP, we found a significant effect of region on pathology burden ( $F = 9.46$ ,  $df = 4,29$ ,  $p < 0.001$ ). Among the 5 core regions sampled, left OFC had the greatest core-region pathology (Fig 3A). Planned post hoc comparisons showed significantly higher burden in left OFC compared to left MFC ( $p < 0.001$ ) and ANG ( $p < 0.001$ ), and in left STG compared to left MFC ( $p = 0.027$ ). In left-hemisphere FTLD-Tau, we found a significant effect of region on cortical pathology ( $F = 7.92$ ,  $df = 4,33$ ,  $p < 0.001$ ). Among the 5 core regions sampled, left MFC had greatest core-region pathology (see Fig 3A). Planned post hoc comparisons showed significantly higher burden in left MFC compared to left OFC ( $p < 0.001$ ), STG ( $p = 0.004$ ), and ANG ( $p = 0.024$ ), and in left ACG compared to left OFC ( $p = 0.006$ ) and STG ( $p = 0.022$ ).

To verify whether these findings were consistent within pathology subtypes, we performed a subanalysis comparing regions of greatest core-region pathology, and found that left OFC was more affected than left MFC in both FTLD-TDP type A/B (beta =  $0.24$ , SE =  $0.02$ ,  $p < 0.001$ ) and type C (beta =  $0.41$ , SE =  $0.08$ ,  $p = 0.008$ ), whereas left MFC was more affected than left OFC in both CBD (beta =  $0.21$ , SE =  $0.05$ ,  $p = 0.023$ ) and PSP (beta =  $0.23$ , SE =  $0.07$ ,  $p = 0.010$ ). We could not perform this subanalysis in PiD because of the limited sample ( $n = 1$ ).

Considering the well-established association between FTLD-TDP and svPPA<sup>2–4</sup> with focal anterior temporal atrophy,<sup>37</sup> we examined the limited left VLT data available in FTLD-TDP ( $n = 4$ ) and found relatively high pathology burden ( $0.76 \pm 0.12$ ).

Although the right hemisphere had less pathology, the findings of greatest core-region pathology were similar to the left hemisphere (see Fig 3B). In FTLD-TDP, region had a significant effect on right-hemisphere pathology ( $F = 4.39$ ,  $df = 4,26$ ,  $p = 0.008$ ), and OFC was the region of greatest core-region pathology in the right hemisphere. Planned post hoc comparisons showed greater burden in right OFC compared to right ANG ( $p = 0.009$ ), and in right ACG compared to right ANG ( $p = 0.019$ ). In FTLD-Tau, right-hemisphere pathology differed by region ( $F = 3.51$ ,  $df = 4,17$ ,  $p = 0.029$ ), and MFC was the region of greatest core-region pathology in the right hemisphere. Although planned post hoc comparisons failed to show significant pairwise contrasts between regions,

we observed a trend for greater pathology in right MFC compared to right OFC ( $p = 0.059$ ).

### **Neuropathological Analysis: Between-Group Comparisons of Pathology Burden**

We directly compared burden in left-hemisphere core-regions with greatest pathology (ie, OFC, MFC) between FTLD-TDP and FTLD-Tau (Fig 4). FTLD-TDP had significantly higher pathology than FTLD-Tau in left OFC (FTLD-TDP =  $0.88 \pm 0.07$ , FTLD-Tau =  $0.57 \pm 0.11$ ;  $F = 47.07$ ,  $df = 1,17$ ,  $p < 0.001$ ), whereas FTLD-Tau had higher pathology in left MFC (FTLD-TDP =  $0.57 \pm 0.09$ , FTLD-Tau =  $0.79 \pm 0.11$ ;  $F = 19.34$ ,  $df = 1,16$ ,  $p < 0.001$ ). In a sub-analysis in pathology subtypes, we found that both FTLD-TDP type A/B and type C had greater pathology in left OFC than CBD ( $p < 0.006$ ) and PSP ( $p < 0.004$ ), whereas CBD and PSP had greater pathology in left MFC than FTLD-TDP type A/B ( $p < 0.03$ ) and type C ( $p < 0.02$ ). In the single PiD patient with left-hemisphere sampling, left MFC burden (0.90) was greater and left OFC burden (0.50) was smaller compared to all individual measurements in FTLD-TDP subtypes. Thus, there was a double dissociation of left-hemisphere pathology, distinguishing OFC as the greatest core-region pathology in FTLD-TDP and MFC as the greatest core-region pathology in FTLD-Tau, consistent across morphological subtypes of these proteinopathies.

### **Clinicopathological Association: Neuroimaging**

We tested the association of postmortem pathology with antemortem cortical thinning in corresponding ROIs in 11 patients with available MRI (FTLD-Tau = 6, FTLD-TDP = 5). Pathology burden was inversely associated with MRI cortical thickness across all available tissue regions and corresponding MRI ROIs (beta =  $-0.04$ , SE = 0.01,  $p = 0.007$ ; Fig 5A). Next, we examined cortical thinning in left-hemisphere ROIs corresponding to the 5 standard core regions to mirror our within-group regional analysis. Among these 5 core ROIs, left OFC was the region of greatest core-region atrophy in FTLD-TDP (mean =  $-3.78 \pm 2.25$ ), whereas left MFC was the region of greatest core-region atrophy in FTLD-Tau (mean =  $-2.10 \pm 1.53$ ). Thus, the antemortem distribution of disease on MRI matched postmortem findings in core regions (see Fig 5B). Similarly, in the right hemisphere, OFC and MFC were the regions of greatest core-region atrophy in FTLD-TDP and FTLD-Tau, respectively (FTLD-TDP right OFC =  $-2.89 \pm 0.80$ ; FTLD-Tau right MFC =  $-2.06 \pm 1.26$ ), consistent with postmortem findings.

### **Clinicopathological Association: Language Features**

Finally, we related the most robust clinical language features, that is, nonfluent speech and single-word comprehension, to

pathology in core-regions with greatest pathology (Fig 6). Across the cohort, patients with early nonfluent speech had higher left MFC burden than patients without such impairment ( $t = -3.62$ ,  $df = 12.00$ ,  $p = 0.004$ ). Patients with early impairment of single-word comprehension showed a trend for greater burden in left OFC ( $t = -2.01$ ,  $df = 7.89$ ,  $p = 0.080$ ). As several patients developed comprehension difficulties only later in the disease (see Table 2), we looked at late impairment (ie, >3 years after onset) of single-word comprehension, and found that it significantly associated with left OFC pathology ( $t = -3.72$ ,  $df = 10.72$ ,  $p = 0.004$ ). We did not find an association of single-word comprehension impairment with left STG pathology ( $p > 0.5$ ), nor did we find an association of right-hemisphere OFC or MFC pathology with single-word comprehension or nonfluent speech, respectively ( $p > 0.05$ ).

Because the left anterior temporal lobe has been implicated in semantic deficits in svPPA<sup>37,38</sup> and we had limited availability of autopsy tissue in this region, we performed an exploratory analysis of a left-hemisphere anterior temporal ROI in antemortem MRI. We found that FTLD-TDP had prominent cortical thinning in left anterior temporal cortex (FTLD-TDP =  $-4.49 \pm 1.53$ ), which did not differ from left OFC cortical thinning in FTLD-TDP ( $t = 1.16$ ,  $df = 4$ ,  $p = 0.310$ ). Left anterior temporal cortical thinning was greater in FTLD-TDP than FTLD-Tau (FTLD-Tau =  $-2.11 \pm 1.66$ ;  $t = -2.47$ ,  $df = 8.86$ ,  $p = 0.036$ ). Finally, MRI cortical thinning was associated with early single-word comprehension deficits in both anterior temporal ( $t = 3.03$ ,  $df = 5.88$ ,  $p = 0.024$ ) and orbitofrontal ( $t = 5.05$ ,  $df = 5.08$ ,  $p = 0.004$ ) cortices.

## **Discussion**

This comparative, bihemispheric, digital pathology study of FTLD-TDP and FTLD-Tau in PPA presents several novel and important findings. First, our digital approach provides expected evidence of left-lateralized pathology in PPA, but some of the observed heterogeneity in laterality may partly be explained by advancing overall dementia severity at end-stage disease (see Fig 2). Next, we find a double dissociation in patterns of cortical pathology in ventral–frontal and temporal regions in FTLD-TDP as opposed to dorsolateral frontal regions in FTLD-Tau (see Figs 3 and 4), and these appear to be common across morphological subtypes of each proteinopathy. Moreover, we find converging evidence for these regional patterns in antemortem MRI, with a direct association between antemortem cortical thinning and postmortem digital pathology (see Fig 5). Finally, this regional susceptibility to distinct proteinopathies directly relates to clinical language features, irrespective of PPA syndromic variants (see Fig 6). We conclude that divergent

TABLE 2. Comparison of Clinical Language Features between FTLD-TDP and FTLD-Tau Groups

Language Features	Early, 0–3 Years			Late, >3 Years		
	FTLD-TDP, n (%)	FTLD-Tau, n (%)	<i>p</i>	FTLD-TDP, n (%)	FTLD-Tau, n (%)	<i>p</i>
Imp single-word retrieval	11/11 (100)	10/10 (100.0)	na	8/8 (100.0)	12/12 (100.0)	na
Imp naming	9/10 (90)	8/9 (88.9)	1.000	8/8 (100.0)	12/12 (100.0)	na
Imp sentence repetition	5/9 (55.6)	3/8 (37.5)	0.637	2/5 (40.0)	11/11 (100.0)	0.018 <sup>a</sup>
Nonfluent speech	4/11 (36.4)	9/10 (90.0)	0.024 <sup>a</sup>	2/8 (25.0)	11/12 (91.7)	0.004 <sup>a</sup>
Agrammatism	4/11 (36.4)	7/10 (70.0)	0.198	1/8 (12.5)	10/12 (83.3)	0.005 <sup>a</sup>
Dysarthria	3/11 (27.3)	5/10 (50.0)	0.387	1/8 (12.5)	8/12 (66.7)	0.028 <sup>a</sup>
Empty speech content	2/11 (18.2)	2/10 (20.0)	1.000	6/8 (75.0)	2/12 (16.7)	0.019 <sup>a</sup>
Semantic paraphasias	5/11 (45.5)	3/10 (30.0)	0.659	5/8 (62.5)	7/12 (58.3)	1.000
Phonemic paraphasias	2/11 (18.2)	5/10 (50.0)	0.183	2/8 (25.0)	10/12 (83.3)	0.019 <sup>a</sup>
Imp gramm compr	6/7 (85.7)	5/10 (50.0)	0.304	3/8 (37.5)	10/12 (83.3)	0.062
Imp single-word compr	7/10 (70)	2/9 (22.2)	0.070	7/7 (100.0)	5/12 (41.7)	0.017 <sup>a</sup>
Imp object knowledge	5/9 (55.6)	2/9 (22.2)	0.335	6/6 (100.0)	3/12 (25.0)	0.009 <sup>a</sup>
Surface dyslexia	1/8 (12.5)	1/9 (11.1)	1.000	4/4 (100.0)	2/7 (28.6)	0.061

Categorical binary clinical features were compared between FTLD-TDP and FTLD-Tau groups using the Fisher exact test independently of clinical phenotype.  
 compr = comprehension; FTLD-Tau = frontotemporal lobar degeneration with inclusions of the tau protein; FTLD-TDP = frontotemporal lobar degeneration with inclusions of the transactive response DNA-binding protein 43; gramm = grammatical; Imp = impaired; na = not available.  
<sup>a</sup>Significant at  $p < 0.05$ .

patterns of cortical pathology in PPA with underlying FTLD-TDP or FTLD-Tau may be helpful to improve antemortem diagnosis of neuropathology based on specific regional burden and associated language features.

Histopathological comparisons across hemispheres in FTLD are very rare due to the lack of bilateral sampling in standard neuropathological protocols.<sup>23,24</sup> Lateralization of postmortem disease has been shown in rare prior postmortem studies, either qualitatively<sup>3</sup> or quantitatively in a small sample of FTLD-TDP.<sup>13–16</sup> Imaging studies suggest that there may be regional specificity to language-related areas in the rate of atrophy progression and lateralization in PPA,<sup>10,11</sup> but these studies lack autopsy data. In our rare bilateral dataset, we found overall left lateralization of cortical pathology in FTLD-TDP and FTLD-Tau, consistent with previous reports.<sup>3,14</sup> Moreover, our digital approach enabled us to detect novel evidence of regional and individual-patient variability (see Fig 2). We observed region-specific lateralization of postmortem pathology in regions with high burden, that is, OFC in FTLD-TDP and MFC in FTLD-Tau, and in a relatively spared region in FTLD-TDP (ie, SPL). In our recent postmortem study in behavioral variant FTD (bvFTD), our digital approach also revealed that lateralization varied

depending on region.<sup>25</sup> Although autopsy data are inherently cross-sectional, our examination of overall dementia severity before autopsy suggests that pathology may become more evenly distributed across hemispheres with advancing disease in PPA. Because all patients had severe language impairment at last visit (score = 3/3 on CDR language subscale), we could not relate laterality to end-stage language impairment specifically, and decreasing lateralization at end-stage disease may reflect the emergence and progression of nonlanguage features captured by the CDR contributing to global disease severity. Although we observed this relationship across FTLD-TDP and FTLD-Tau, FTLD proteinopathies may differ in the rate of neurodegeneration,<sup>39</sup> and future work will help clarify the progression of lateralization in these pathologies. In our study, FTLD-TDP and FTLD-Tau had divergent regional distributions of postmortem pathology, which were consistent across hemispheres and among morphological subtypes of each proteinopathy. FTLD-TDP had greatest core-region pathology in left OFC. Postmortem work identifies OFC as a likely site of early TDP-43 pathology in bvFTD.<sup>40</sup> We are unaware of any large-scale study of regional TDP-43 distribution specifically in PPA, yet one reported PPA patient with *GRN* mutation showed relatively high TDP-43 counts in OFC.<sup>13</sup>



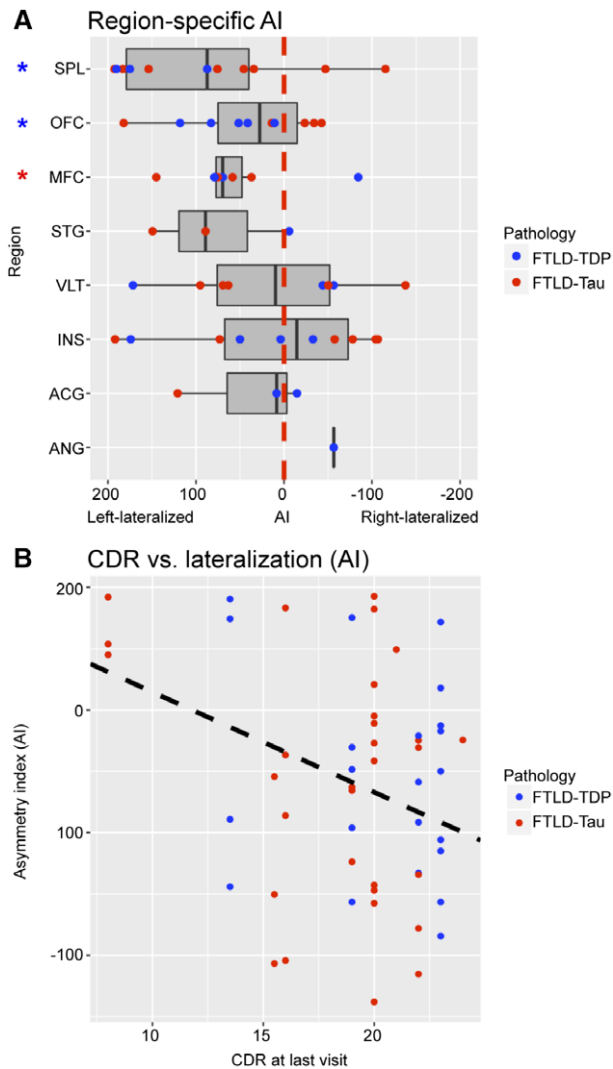


**FIGURE 2: Region-specific lateralization of cortical disease and association with clinical dementia severity.** (A) Box-plots depict asymmetry index (AI) values calculated in available bilaterally sampled region-pairs. An AI greater than zero (on the left side of the red dashed line) indicates left lateralization of pathology burden. Overall, we find left lateralization of cortical pathology in both frontotemporal lobar degeneration (FTLD) with inclusions of the transactive response DNA-binding protein 43 (FTLD-TDP) and FTLD with inclusions of the tau protein (FTLD-Tau), but individual and regional patient data may have variable degrees of hemispheric laterality. In FTLD-TDP, orbitofrontal cortex (OFC) and superior parietal lobule (SPL) are significantly left-lateralized (ie, asymmetry index  $>0$ ;  $p < 0.05$ ); in FTLD-Tau, midfrontal cortex (MFC) is significantly left-lateralized ( $p < 0.05$ ). Blue asterisks indicate significant findings in FTLD-TDP, whereas the red asterisk indicates a significant finding in FTLD-Tau. ACG = anterior cingulate gyrus; ANG = angular gyrus; INS = insular cortex; STG = superior-temporal gyrus; VLT = ventrolateral temporal cortex. (B) Scatterplot shows an inverse linear relationship between clinical dementia severity proximal to autopsy and degree of lateralization (ie, AI) across all bilaterally sampled regions ( $\beta = -8.18$ , standard error = 3.22,  $p = 0.015$ ). Data were analyzed using linear mixed effects analysis to account for interdependency of multiple measurements from the same individuals. CDR = Clinical Dementia Rating including frontotemporal dementia subfields.<sup>32</sup>

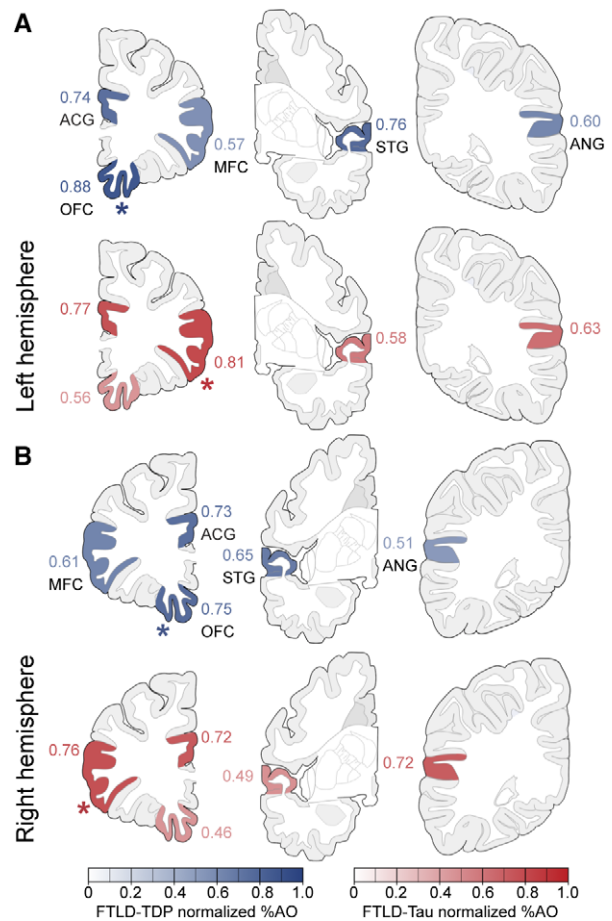


**FIGURE 3: Regional distribution of pathology in five standard core regions in frontotemporal lobar degeneration (FTLD) with inclusions of the transactive response DNA-binding protein 43 (FTLD-TDP) and FTLD with inclusions of the tau protein (FTLD-Tau) in left and right hemispheres.** Heat-map portrays regional distribution of cortical pathology in left and right hemispheres in FTLD-TDP (blue) and FTLD-Tau (red). Here we display regional least-square means of normalized percentage area occupied by pathology after normalization [0;1] (%AO) from linear mixed effects within-group regional analysis in 5 standard core regions. (A) In the left hemisphere, we found greatest core-region pathology in left orbitofrontal cortex (OFC) in FTLD-TDP and left right midfrontal cortex (MFC) in FTLD-Tau. (B) In the right hemisphere, we found similar findings of greatest core-region pathology in right OFC in FTLD-TDP and MFC in FTLD-Tau. Regions of greatest core-region pathology in each hemisphere are marked with an asterisk. ACG = anterior cingulate gyrus; ANG = angular gyrus; STG = superior-temporal gyrus.

TDP-43 copathology may occur in aged AD or cognitively normal patients, and relatively mild TDP-43 pathology is found in OFC,<sup>41</sup> as opposed to our data in PPA and in our previous study of bvFTD.<sup>25</sup> This suggests that TDP-43 copathology in advanced aging may be distinct from primary TDP-43 pathology in FTLD. Although our findings point to OFC as a key disease area in PPA with FTLD-TDP, we had limited tissue outside of our core-regions, and we cannot exclude anterior temporal regions having high TDP-43 burden. We found preliminary evidence of relatively high

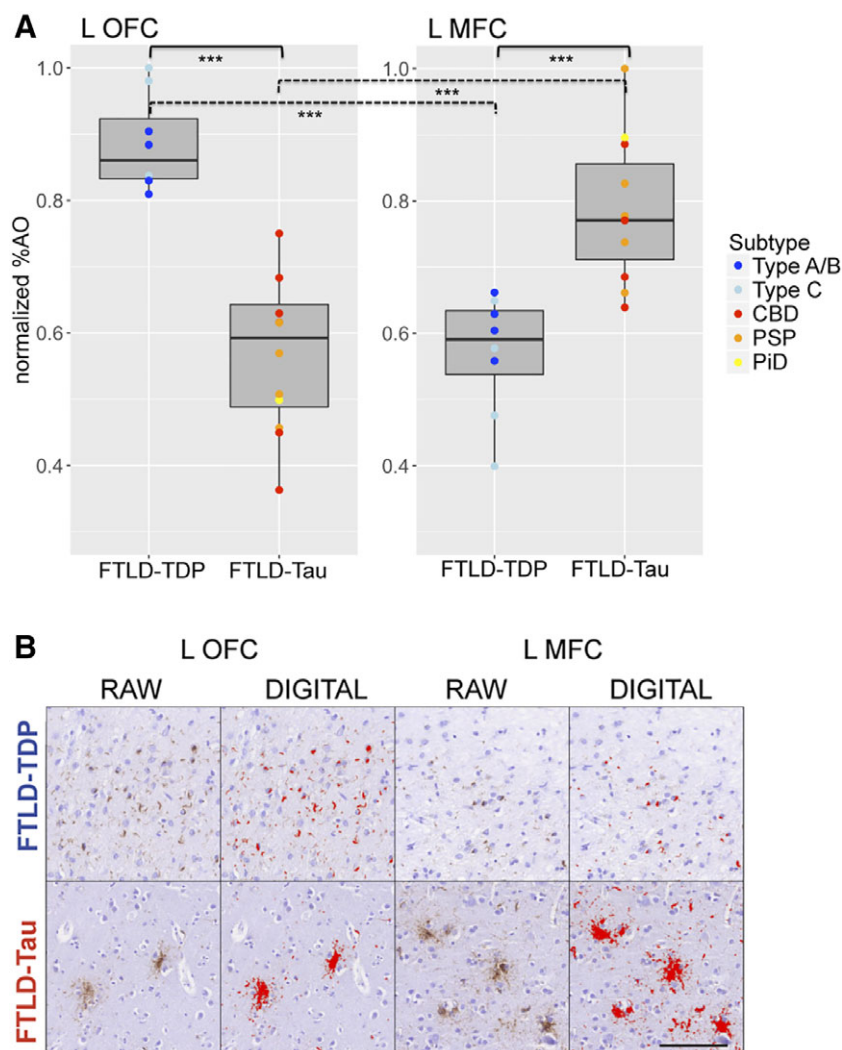


**FIGURE 4:** Regional comparisons of cortical neuropathological burden in greatest core-region pathology regions. (A) Boxplots portray direct within-group and between-group comparisons of cortical pathology (ie, normalized percentage area occupied by pathology after normalization [0;1] [%AO]) in greatest core-region pathology regions. Within frontotemporal lobar degeneration (FTLD) with inclusions of the transactive response DNA-binding protein 43 (FTLD-TDP), left (L) orbitofrontal cortex (OFC) had greater pathology than left midfrontal cortex (MFC;  $p < 0.001$ ), whereas within FTLD with inclusions of the tau protein (FTLD-Tau), left MFC had greater pathology than left OFC ( $p < 0.001$ ). Between pathologies, FTLTDP had greater pathology in left OFC than FTLT-Tau (mean FTLTDP =  $0.88 \pm 0.07$ ; mean FTLT-Tau =  $0.57 \pm 0.11$ ;  $F = 47.07$ ,  $df = 1,17$ ,  $p < 0.001$ ), whereas FTLT-Tau had greater pathology in left MFC than FTLTDP (mean FTLTDP =  $0.57 \pm 0.09$ ; mean FTLT-Tau =  $0.79 \pm 0.11$ ;  $F = 19.34$ ,  $df = 1,16$ ,  $p < 0.001$ ). Subanalyses showed consistent results across pathology subtypes. Here, digital pathology measurements are color-coded by pathology subtypes. Significant findings with  $p < 0.001$  are marked with 3 asterisks. Type A/B and type C are FTLTDP subtypes. CBD = corticobasal degeneration; PiD = Pick disease; PSP = progressive supranuclear palsy. (B) Images show pathology burden in left OFC and left MFC comparatively in a case of FTLTDP type A with a *GRN* mutation and clinical semantic primary progressive aphasia and in a case of FTLT-Tau PSP with nonfluent/agrammatic primary progressive aphasia (scale bar = 100  $\mu\text{m}$ ). We include both raw images with immunohistochemical staining of TDP-43 (rat monoclonal TAR5P-1D3, p409/410, Ascension)<sup>27</sup> and tau (AT8, Millipore),<sup>28</sup> as well as digital images with thresholding parameters for digital detection of TDP-43 and tau inclusions. Whereas the FTLTDP case has relatively high burden of TDP-43 inclusions in OFC and relatively low burden in MFC, the FTLT-Tau case has relatively low burden of tau inclusions in OFC and relatively high burden in MFC.

pathology in left VLT ( $0.76 \pm 0.12$ ) in our limited sample with available tissue ( $n = 4$ ) that was similar to mean TDP-43 burden in left OFC (see Fig 3), but a larger sample would be necessary to more reliably assess pathology burden in this area. Relatively high temporal burden in FTLTDP was also found in left STG (see Fig 3A), yet this region is more posterior compared to areas typically associated with semantic

knowledge in PPA.<sup>38,42</sup> Nevertheless, with increasing severity, the distribution of pathology may spread from anterior temporal to more posterior temporal regions.<sup>9</sup>

FTLT-Tau is known to affect frontal areas,<sup>43</sup> but regional burden of FTLT-Tau in PPA is understudied. In a cohort of PiD, mostly with clinical bvFTD, we found the highest levels of pathology in frontal and limbic

regions.<sup>31</sup> Furthermore, significant frontal disease in PSP has been linked to cognitive features.<sup>44</sup> Here, FTLN-Tau showed greatest core-region pathology in MFC bilaterally, greater in the left hemisphere than the right hemisphere, consistent with the idea that both frontal cortices may contribute to language deficits in naPPA.<sup>12</sup> However, only left-hemisphere MFC burden directly associated with nonfluent speech. We cannot, however, rule out other indirect contributions of right-hemisphere disease to language deficits, or the involvement of other regions outside of our sampling.

Regional patterns of specific proteinopathies likely influence the clinical manifestations of PPA. In our cohort, 8 of 9 svPPA patients had FTLN-TDP pathology, whereas 10 of 13 naPPA patients had FTLN-Tau pathology. Although this is consistent with previous associations,<sup>2</sup> a considerable subset of the cohort (19%) was unclassifiable due to concurrent nonfluent/agrammatic and semantic features (2/5 FTLN-TDP, 3/5 FTLN-Tau), similar to previous reports of PPA with mixed features.<sup>3,4</sup> Due to these ambiguities of PPA syndromic variants,<sup>7</sup> we compared specific language features between proteinopathies irrespective of clinical syndromes. We found a double dissociation, with greater single-word comprehension difficulties in FTLN-TDP as opposed to nonfluent speech in FTLN-Tau (see Table 2), and this was associated with increased burden in specific neuroanatomical regions, that is, left OFC and left MFC, respectively. Distinct regional patterns of FTLN-TDP and FTLN-Tau (see Figs 3 and 4) thus directly relate to language deficits (see Fig 6).

Consider first semantic deficits in FTLN-TDP. Left OFC burden, prominent in FTLN-TDP, was associated with antemortem semantic difficulties across the cohort. OFC may play a specific role in the semantic network such as lexical search<sup>45</sup>; orbitofrontal areas have been implicated in semantic studies in svPPA and bvFTD,<sup>37,46</sup> and atrophy in svPPA has been shown to extend to OFC.<sup>9</sup> Additionally, the left uncinate fasciculus connecting anterior temporal and ventral-frontal areas may contribute to semantic retrieval and semantic association tasks.<sup>47</sup> Although we had limited anterior temporal tissue (ie, VLT), in antemortem MRI we found an association of anterior temporal and orbitofrontal atrophy, greater in FTLN-TDP, with single-word comprehension difficulties. Thus, alongside the anterior temporal cortex, OFC appears to be intimately associated with TDP-43 pathology and may contribute to semantic deficits in PPA. By comparison, patients with nonfluent speech had greater left MFC pathology than patients with intact fluency, consistent with previous antemortem work.<sup>12,48,49</sup> We could not test the reported association between nonfluent speech and left INS pathology<sup>12</sup> in our dataset due to limited data in this region. However, our findings of a double dissociation in language features between

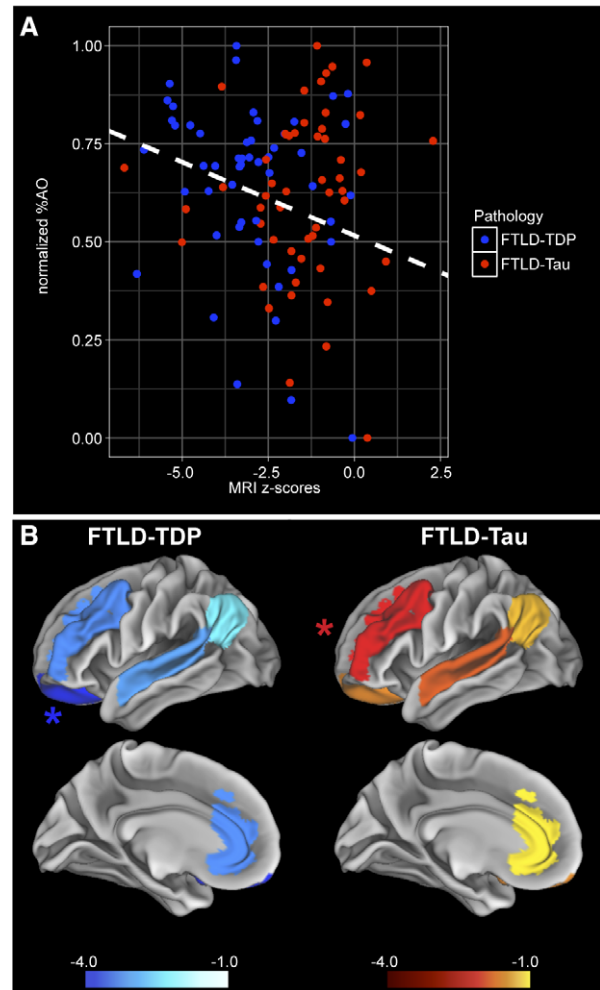


**FIGURE 5:** Magnetic resonance imaging (MRI) cortical thinning is reflective of cortical neuropathological burden at autopsy. (A) Scatterplot portrays a significant negative relationship between pathology burden (ie, normalized percentage area occupied by pathology after normalization [0;1] [%AO]) and cortical thickness z scores from antemortem MRI in regions matching autopsy sampling across pathology groups (beta =  $-0.04$ , standard error =  $0.01$ ,  $p = 0.007$ ). The fit line represents the linear association between cortical thickness z scores (x-axis) and normalized %AO (y-axis) in corresponding regions, and has been derived in a linear mixed effects model<sup>36</sup> accounting for multiple measurements from the same patient as well as 1 covariate (ie, time from scan to autopsy), which may confound the linear association between the 2 measurements. Data points are color-coded by pathology (ie, frontotemporal lobar degeneration [FTLD] with inclusions of the transactive response DNA-binding protein 43 [FTLD-TDP] = blue, FTLD with inclusions of the tau protein [FTLD-Tau] = red). (B) Heat-map shows relative MRI cortical thinning in left-hemisphere regions of interest (ROIs) matching 5 standard core regions sampled at autopsy in FTLN-TDP and FTLN-Tau. Regions are color-coded by relative severity of cortical thinning as compared to healthy controls (scale bars = z scores) within pathology groups. Group means are obtained from 11 patients (5 FTLN-TDP, 6 FTLN-Tau) with available antemortem structural MRI. Among these core ROIs, FTLN-TDP has greatest core-region atrophy in left orbitofrontal cortex (mean =  $-3.78 \pm 2.25$ ), whereas FTLN-Tau has greatest core-region atrophy in left midfrontal cortex (mean =  $-2.10 \pm 1.53$ ), validating our postmortem findings. Regions of greatest core-region atrophy are marked with an asterisk.

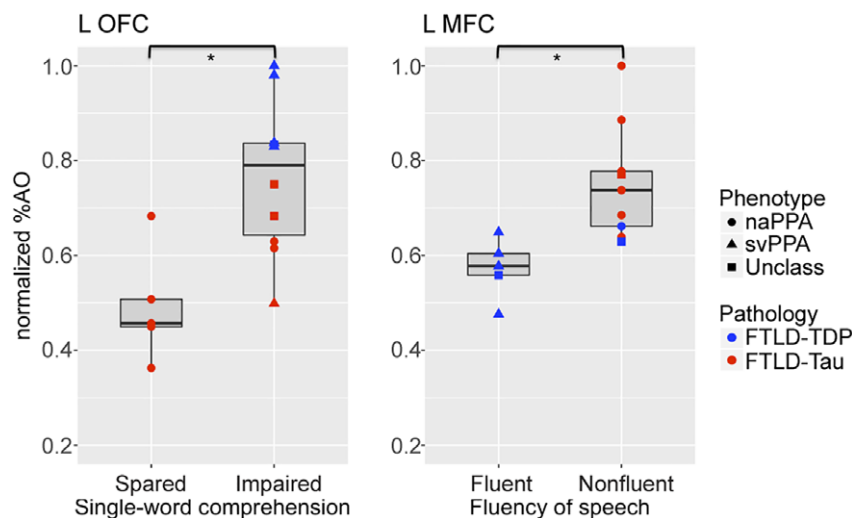


**FIGURE 6:** Clinicopathological associations of left-hemisphere greatest core-region pathology regions with clinical language features. Boxplots show correlations of cortical pathology burden (ie, normalized percentage area occupied by pathology after normalization [0;1] [%AO]) in greatest core-region pathology regions with clinical language features. Data points are color-coded by pathology group (ie, frontotemporal lobar degeneration [FTLD] with inclusions of the transactive response DNA-binding protein 43 [FTLD-TDP] = blue, FTLD with inclusions of the tau protein [FTLD-Tau] = red) and shape-coded by clinical phenotype (ie, circle = nonfluent/agrammatic primary progressive aphasia [naPPA], triangle = semantic primary progressive aphasia [svPPA], square = unclassifiable with mixed features). Irrespective of primary progressive aphasia clinical variant, patients with single-word comprehension impairment in late disease (ie, >3 years after onset) had more severe cortical disease in left (L) orbitofrontal cortex (OFC) than patients with sparing of this language function ( $t = -3.72$ ,  $df = 10.72$ ,  $p = 0.004$ ); patients with nonfluent speech in early disease (ie, 0–3 years after onset) had more severe cortical disease in left midfrontal cortex (MFC) than patients with fluent speech ( $t = -3.62$ ,  $df = 12.00$ ,  $p = 0.004$ ). Statistical significance ( $p < 0.05$ ) is indicated with an asterisk. Unclass = unclassifiable primary progressive aphasia with concurrent nonfluent/agrammatic and semantic features.

FTLD-TDP and FTLT-Tau highlight the potential role of these linguistic features that can serve as inexpensive screening tools for diagnostic markers that predict pathology in PPA, while avoiding some of the ambiguities associated with syndromic variants.<sup>50</sup>

This is, to our knowledge, the first attempt to integrate evidence from antemortem MRI with postmortem pathology in PPA. We found that pathology measurements are reflected in the degree of antemortem cortical thinning during life in corresponding regions, while accounting for the time period between scanning and autopsy. Greatest core-region pathology regions in FTLT-TDP and FTLT-Tau corresponded to areas of greatest core-region atrophy on MRI, in both left and right hemispheres. Our study in bvFTD also associated regional pathologic burden with antemortem MRI cortical thinning<sup>25</sup>; this was achievable partly because of our digital histopathological approach. These novel findings of concordance between postmortem pathology and antemortem atrophy are an important first step for pathologic-imaging validation in PPA, and provide proof-of-concept evidence that tissue-guided imaging approaches may eventually help establish diagnostic biomarkers during life.

Some caveats should be considered when interpreting these data. We had insufficient harmonized neuropsychological assessments for quantitative analysis of language and had missing data for some patients; however, we used a validated

chart extraction method including a consensus panel, most patients had detailed longitudinal assessments with structured language evaluations, and > 75% were seen within 3 years of onset. Comprehensive standardized neuropsychological assessments in PPA patients followed to autopsy are needed to confirm our clinicopathological associations. Although we have strong rationale to compare FTLT-TDP and FTLT-Tau based on current nomenclature<sup>23</sup> and shared genetic risk,<sup>51,52</sup> our cohort was neuropathologically and genetically diverse. The few *GRN* carriers and left-handed individuals did not appear to deviate substantially from typical PPA with FTLT-TDP and FTLT-Tau. We carefully identified patients with a monoproteinopathy, not confounded by vascular or significant AD copathology. Although we were underpowered to evaluate all genetic and pathological subgroups, we accounted for morphological differences by normalizing %AO measurements within proteinopathy subtypes, and subanalyses in these subtypes showed consistent findings (see Fig 4). We performed rigorous validation of our digital algorithms and sampling approach<sup>22</sup> to minimize (pre-)analytical bias. Due to the rarity of antemortem research-quality MRI in autopsy cohorts, our MRI subset was relatively small ( $n = 11$ ). Finally, although we sampled several “extended” regions important for FTLT, this represents only an approximation of the widespread language network described in whole-brain neuroimaging.<sup>8,9,12</sup> Therefore, other regions in the language network,

such as the left anterior temporal lobe, may show stronger associations with semantic comprehension and TDP-43 pathology in future studies.

With these limitations in mind, we demonstrate that postmortem pathology is left-lateralized in PPA regardless of underlying pathology, that lateralization diminishes with increasingly severe dementia, that FTLD-TDP and FTLD-Tau have doubly-dissociated, pathology-specific patterns of disease, and that the anatomic distribution of pathology is related to distinct antemortem linguistic and imaging features in FTLD-TDP and FTLD-Tau with clinical PPA. We thus propose that distinct FTLD proteinopathies underlying PPA may eventually be detected during life with the help of tissue-guided imaging and neuropsychological linguistic markers reflecting divergent microscopic patterns of TDP-43 and tau.

---

## Acknowledgment

This study was supported by NIH grants AG017586, AG038490, AG052943, AG054519, AG010124, AG043503, and by NINDS NS088341, the Penn Institute on Aging, an anonymous donor, and the Wyncote Foundation. Alzheimer Nederland and the Royal Netherlands Academy of Arts and Sciences (Van Walree Grant) supported L.A.A.G. with student travel funding.

We thank the patients and their families for their participation in medical research; M. Neumann and E. Kremmer for providing the phosphorylation-specific TDP-43 antibody p409/410; M. Leonard for her assistance in the creation of Figure 3; and C. Olm and P. Ferraro for their assistance in the creation of Figure 5B.

## Author Contributions

L.A.A.G., M.G., and D.J.I. contributed to the conception and design of the study; all authors contributed to the acquisition and analysis of data; L.A.A.G., M.G., and D.J.I. contributed to drafting the text and preparing the figures.

## Potential Conflicts of Interest

Nothing to report.

---

## References

- Mesulam MM. Primary progressive aphasia. *Ann Neurol* 2001;49:425–432.
- Grossman M. Primary progressive aphasia: clinicopathological correlations. *Nat Rev* 2010;6:88–97.
- Mesulam MM, Weintraub S, Rogalski EJ, et al. Asymmetry and heterogeneity of Alzheimer's and frontotemporal pathology in primary progressive aphasia. *Brain* 2014;137:1176–1192.
- Giannini LAA, Irwin DJ, McMillan CT, et al. Clinical marker for Alzheimer disease pathology in logopenic primary progressive aphasia. *Neurology* 2017;88:2276–2284.
- Spinelli EG, Mandelli ML, Miller ZA, et al. Typical and atypical pathology in primary progressive aphasia variants. *Ann Neurol* 2017;81:430–443.
- Alladi S, Xuereb J, Bak T, et al. Focal cortical presentations of Alzheimer's disease. *Brain* 2007;130(pt 10):2636–2645.
- Gorno-Tempini ML, Hillis AE, Weintraub S, et al. Classification of primary progressive aphasia and its variants. *Neurology* 2011;76:1006–1014.
- Mandelli ML, Vilaplana E, Brown JA, et al. Healthy brain connectivity predicts atrophy progression in non-fluent variant of primary progressive aphasia. *Brain* 2016;139(pt 10):2778–2791.
- Collins JA, Montal V, Hochberg D, et al. Focal temporal pole atrophy and network degeneration in semantic variant primary progressive aphasia. *Brain* 2017;140:457–471.
- Rohrer JD, Clarkson MJ, Kittur R, et al. Rates of hemispheric and lobar atrophy in the language variants of frontotemporal lobar degeneration. *J Alzheimers Dis* 2012;30:407–411.
- Rogalski E, Cobia D, Martersteck A, et al. Asymmetry of cortical decline in subtypes of primary progressive aphasia. *Neurology* 2014;83:1184–1191.
- Grossman M, Powers J, Ash S, et al. Disruption of large-scale neural networks in non-fluent/agrammatic variant primary progressive aphasia associated with frontotemporal degeneration pathology. *Brain Lang* 2013;127:106–120.
- Gliebus G, Bigio EH, Gasho K, et al. Asymmetric TDP-43 distribution in primary progressive aphasia with progranulin mutation. *Neurology* 2010;74:1607–1610.
- Kim G, Ahmadian SS, Peterson M, et al. Asymmetric pathology in primary progressive aphasia with progranulin mutations and TDP inclusions. *Neurology* 2016;86:627–636.
- Kim G, Vahedi S, Gefen T, et al. Asymmetric TDP pathology in primary progressive aphasia with right hemisphere language dominance. *Neurology* 2018;90:e396–e403.
- Kim G, Bolbolan K, Gefen T, et al. Atrophy and microglial distribution in primary progressive aphasia with TDP-43. *Ann Neurol* 2018;83:1096–1104.
- Nevler N, Ash S, Irwin DJ, et al. Validated automatic speech biomarkers in primary progressive aphasia. *Ann Clin Transl Neurol* 2018;6:4–14.
- Josephs KA, Martin PR, Botha H, et al. [18F]AV-1451 tau-PET and primary progressive aphasia. *Ann Neurol* 2018;83:599–611.
- Santos-Santos MA, Mandelli ML, Binney RJ, et al. Features of patients with nonfluent/agrammatic primary progressive aphasia with underlying progressive supranuclear palsy pathology or corticobasal degeneration. *JAMA Neurol* 2016;73:733–742.
- Xie SX, Baek Y, Grossman M, et al. Building an integrated neurodegenerative disease database at an academic health center. *Alzheimers Dement* 2011;7:e84–e93.
- Toledo JB, Van Deerlin VM, Lee EB, et al. A platform for discovery: the University of Pennsylvania Integrated Neurodegenerative Disease Biobank. *Alzheimers Dement* 2014;10:477–484.e1.
- Irwin DJ, Byrne MD, McMillan CT, et al. Semi-automated digital image analysis of Pick's disease and TDP-43 proteinopathy. *J Histochem Cytochem* 2016;64:54–66.
- Mackenzie IR, Neumann M, Bigio EH, et al. Nomenclature and nosology for neuropathologic subtypes of frontotemporal lobar degeneration: an update. *Acta Neuropathol* 2010;119:1–4.
- Montine TJ, Phelps CH, Beach TG, et al. National Institute on Aging-Alzheimer's Association guidelines for the neuropathologic

- assessment of Alzheimer's disease: a practical approach. *Acta Neuropathol* 2012;123:1–11.
25. Irwin DJ, McMillan CT, Xie SX, et al. Asymmetry of post-mortem neuropathology in behavioural-variant frontotemporal dementia. *Brain* 2018;141:288–301.
  26. Wood EM, Falcone D, Suh E, et al. Development and validation of pedigree classification criteria for frontotemporal lobar degeneration. *JAMA Neurol* 2013;70:1411–1417.
  27. Neumann M, Kwong LK, Lee EB, et al. Phosphorylation of S409/410 of TDP-43 is a consistent feature in all sporadic and familial forms of TDP-43 proteinopathies. *Acta Neuropathol* 2009;117:137–149.
  28. Mercken M, Vandermeeren M, Lübke U, et al. Monoclonal antibodies with selective specificity for Alzheimer tau are directed against phosphatase-sensitive epitopes. *Acta Neuropathol* 1992;84:265–272.
  29. Libon DJ, Rascovsky K, Gross RG, et al. The Philadelphia Brief Assessment of Cognition (PBAC): a validated screening measure for dementia. *Clin Neuropsychol* 2011;25:1314–1330.
  30. Avants BB, Libon DJ, Rascovsky K, et al. Sparse canonical correlation analysis relates network-level atrophy to multivariate cognitive measures in a neurodegenerative population. *Neuroimage* 2014;84:698–711.
  31. Irwin DJ, Brettschneider J, McMillan CT, et al. Deep clinical and neuropathological phenotyping of Pick disease. *Ann Neurol* 2016;79:272–287.
  32. Knopman DS, Weintraub S, Pankratz VS. Language and behavior domains enhance the value of the clinical dementia rating scale. *Alzheimer's Dement* 2011;7:293–299.
  33. Avants BB, Tustison NJ, Song G, et al. A reproducible evaluation of ANTs similarity metric performance in brain image registration. *Neuroimage* 2011;54:2033–2044.
  34. Tustison NJ, Cook PA, Klein A, et al. Large-scale evaluation of ANTs and FreeSurfer cortical thickness measurements. *Neuroimage* 2014;99:166–179.
  35. Wang H, Yushkevich PA. Multi-atlas segmentation with joint label fusion and corrective learning—an open source implementation. *Front Neuroinform* 2013;7:27.
  36. Laird NM, Ware JH. Random-effects models for longitudinal data. *Biometrics* 1982;38:963–974.
  37. Mummery CJ, Patterson K, Price CJ, et al. A voxel-based morphometry study of semantic dementia: relationship between temporal lobe atrophy and semantic memory. *Ann Neurol* 2000;47:36–45.
  38. Mesulam MM, Wieneke C, Hurlley R, et al. Words and objects at the tip of the left temporal lobe in primary progressive aphasia. *Brain* 2013;136:601–618.
  39. Whitwell JL, Boeve BF, Weigand SD, et al. Brain atrophy over time in genetic and sporadic frontotemporal dementia: a study of 198 serial magnetic resonance images. *Eur J Neurol* 2015;22:745–752.
  40. Brettschneider J, Del Tredici K, Irwin DJ, et al. Sequential distribution of pTDP-43 pathology in behavioral variant frontotemporal dementia (bvFTD). *Acta Neuropathol* 2014;127:423–439.
  41. Nag S, Yu L, Boyle PA, et al. TDP-43 pathology in anterior temporal pole cortex in aging and Alzheimer's disease. *Acta Neuropathol Commun* 2018;6:33.
  42. Bonner MF, Price AR, Peelle JE, Grossman M. Semantics of the visual environment encoded in parahippocampal cortex. *J Cogn Neurosci* 2016;28:361–378.
  43. Kovacs GG. Invited review: Neuropathology of tauopathies: principles and practice. *Neuropathol Appl Neurobiol* 2015;41:3–23.
  44. Josephs KA, Boeve BF, Duffy JR, et al. Atypical progressive supranuclear palsy underlying progressive apraxia of speech and non-fluent aphasia. *Neurocase* 2005;11:283–296.
  45. Thompson-Schill SL. Neuroimaging studies of semantic memory: inferring "how" from "where." *Neuropsychologia* 2003;41:280–292.
  46. Cousins KA, York C, Bauer L, Grossman M. Cognitive and anatomic double dissociation in the representation of concrete and abstract words in semantic variant and behavioral variant frontotemporal degeneration. *Neuropsychologia* 2016;84:244–251.
  47. Grossman M, McMillan C, Moore P, et al. What's in a name: voxel-based morphometric analyses of MRI and naming difficulty in Alzheimer's disease, frontotemporal dementia and corticobasal degeneration. *Brain* 2004;127:628–649.
  48. Ash S, Moore P, Vesely L, et al. Non-fluent speech in frontotemporal lobar degeneration. *J Neurolinguistics* 2009;22:370–383.
  49. Gunawardena D, Ash S, McMillan C, et al. Why are patients with progressive nonfluent aphasia nonfluent? *Neurology* 2010;75:588–594.
  50. Grossman M. Linguistic aspects of primary progressive aphasia. *Annu Rev Linguist* 2018;4:377–403.
  51. Van Deerlin VM, Sleiman PMA, Martinez-Lage M, et al. Common variants at 7p21 are associated with frontotemporal lobar degeneration with TDP-43 inclusions. *Nat Genet* 2010;42:234–239.
  52. Kouri N, Ross OA, Dombroski B, et al. Genome-wide association study of corticobasal degeneration identifies risk variants shared with progressive supranuclear palsy. *Nat Commun* 2015;6:7247.